An avascular tumour growth model with random variation

Ang Keng Cheng[1] and Tan Liang Soon[2]

National Institute of Education
Nanyang Technological University
1, Nanyang Walk
Singapore 637616
[1]kcang@nie.edu.sg [2]shan@ri.sch.edu.sg

Abstract

A mathematical model is developed to describe the processes of avascular tumour growth. The tumour is treated on a macroscopic perspective, in which the spatio-temporal dynamics of cell concentrations are modelled based on reaction-diffusion dynamics and mass conservation law. Novel features of the model include the dependence of the cell proliferation rate on the growth inhibiting factors secreted by necrotic cells and the incorporation of random variation to the mitotic rate and nutrient supply. It is assumed that these random components play an important role in the tumour's asymmetric growth. With the aid of computational technology, numerical techniques are used to investigate the growth patterns of the proliferating, quiescent and necrotic cell densities in response to changes in various model parameters. The biological and clinical implications of these results are discussed.

1 Introduction

The development of a primary solid tumour begins with a single normal cell becoming transformed as a result of mutations in certain key genes. This transformed cell differs from a normal one in its escape from the body's homeostatic mechanisms, leading to inappropriate proliferation and a tendency to override apoptosis. An individual tumour cell has the potential, over successive divisions, to develop into a cluster of tumour cells. Further growth and proliferation leads to the development of an avascular tumour consisting of approximately 10^6 cells which feed on oxygen and other nutrients present in the local environment.

After the early stages of growth, the avascular spheroids consist structurally of an inner zone of necrotic cells (dead due to lack of nutrients) and an outer zone of living cells. This outer zone can be further divided into a layer largely composed of quiescent cells and a layer largely composed of proliferating cells, although dead cells are also found adjacent to both quiescent and proliferating cells (Sutherland, 1988). At this stage the spheroids tend to reach a finite size of at most a few millimetres in diameter (Folkman and Hochberg, 1973). In this state of

"dynamic equilibrium" there is a balance between mitosis and the death and disintegration of tumour cells into waste products, mainly water.

Mechanical effects from the surrounding environment as well as that generated internally by cellular growth have been shown to play an important role in regulating tumour growth. Evidence that cell stress affects proliferation is provided by Helmlinger *et al.* (1997). In culturing spheroids in gels of different stiffness, it was demonstrated that the stress exerted on tumour cells by their surroundings affects its equilibrium size.

In recent years several mathematical models, using different approaches, have been developed to describe the features of avascular tumour growth. Following experimental observations that the transitions between layers of tumour cells are more likely to be gradual than sharp (Hystad and Rofstad, 1994), some of these models have used a continuum, macroscopic framework in one space dimension (Ward and King, 1997, 1999). Sherratt and Chaplain (2001) have examined the implications of incorporating random cell movement into the continuum of live tumour cells on avascular tumour growth.

A common feature of the models described above is that they have assumed that the tumour cells are of the same type for the simplicity of closing the system of mass balance equations. This approach does not permit the investigation of the chematic effects that different clones of cells (for example, cells with different expression of the tumour suppressor gene p53) have on the morphology of the vascular environment, and hence, the nutrient supply.

In this paper, we attempt to develop a mathematical description of avascular tumour growth *in vivo* on a continuum model, taking into account the random effects that cellular stress and the disparate clones of cells may have on the mitotic rate and nutrient level respectively. We also include the effects of mitotic inhibitors based on the experimental observation that growth saturation in multicellular tumour spheroids is regulated by factors produced, released, or activated during the process of necrosis (Freyer, 1988).

2 Model Formulation

The mathematical model that we describe is essentially based on the modelling framework presented in Sherratt & Chaplain. As can be seen from the schematic diagram presented in Figure 1, the *in vivo* tumour is treated as a continuum of proliferating, quiescent and necrotic cells, whose densities are denoted by $p(x,t)$, $q(x,t)$ and $n(x,t)$ respectively, where t and x are the time and the one dimensional spatial coordinate respectively.

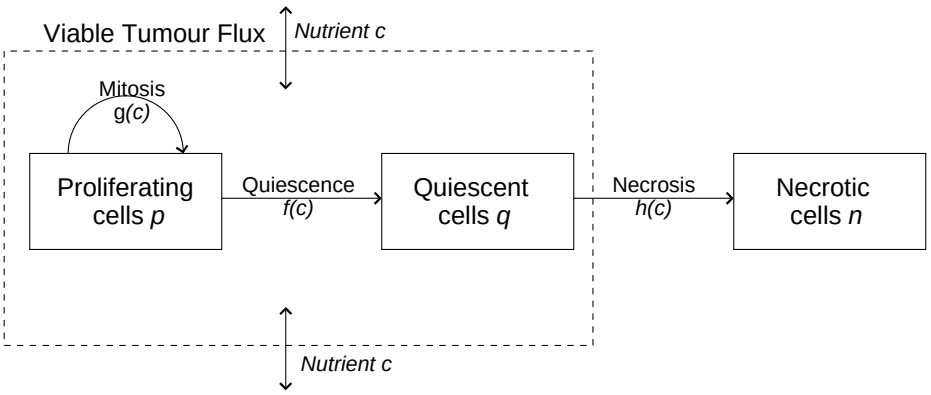

Figure 1: A schematic diagram of the interaction between the proliferating, quiescent and necrotic cell densities

In the model developed by Sherratt & Chaplain, the mitosis rate $g(c)$ of the proliferating cells is assumed to be proportional to the concentration $c(x,t)$ of nutrients and limited by the crowding effects of the total cell population. The nutrients is assumed to pass through the surface of the tumour and diffuse into the interior through the intracellular space sufficiently fast enough that the local nutrient concentration $c(x,t)$ is quasi steady. In the direction of the core of the tumour, some proliferating cells with limited access to the intracellular nutrients become quiescent at rate $f(c)$ and some quiescent cells which are totally deprived of nutrients undergo necrosis at rate $h(c)$.

In order to include the phenomenological factor of contact inhibition in the random motility of tumour cells, the overall viable cell flux $\dfrac{\partial}{\partial x}(p+q)$ as illustrated in Figure 1 is fractionated evenly between the proliferating and quiescent cells densities. This is based on the assumption that the two cell populations have equal motility. The movement terms of the proliferating and quiescent cells are in turn given by $\dfrac{\partial}{\partial x}\left[\dfrac{p}{p+q}\dfrac{\partial(p+q)}{\partial x}\right]$ and $\dfrac{\partial}{\partial x}\left[\dfrac{q}{p+q}\dfrac{\partial(p+q)}{\partial x}\right]$ respectively.

With mass conservation applied to the cells, the set of Sherratt and Chaplain's equations governing the evolution of $p(x,t)$, $q(x,t)$, $n(x,t)$ and $c(x,t)$ are presented in turn below.

$$\frac{\partial p}{\partial t} = \frac{\partial}{\partial x}\left[\frac{p}{p+q}\frac{\partial(p+q)}{\partial x}\right] + g(c)p(1-p-q-n) - f(c)p \tag{1}$$

$$\frac{\partial q}{\partial t} = \frac{\partial}{\partial x}\left[\frac{q}{p+q}\frac{\partial(p+q)}{\partial x}\right] + f(c)p - h(c)q \tag{2}$$

$$\frac{\partial n}{\partial t} = h(c)q \tag{3}$$

$$c = \frac{c_0\gamma}{\gamma+p}\left[1-\alpha\left(p+q+n\right)\right] \tag{4}$$

Equation (4) represents the access of nutrient from underlying tissue. By assuming that the effectiveness of this source term decreases with overall cell density, the parameter $\alpha \in (0,1]$ represents a constant of proportionality and c_0 is the nutrient concentration in the absence of a tumour cell population. It is assumed that the cells are completely closed-packed at the maximum non-dimensionalised cell density of 1. Moreover, the functions $f(c)$ and $h(c)$ are assumed to be decreasing with $f\left(+\infty\right) = h\left(+\infty\right) = 0$.

To render the description of the dynamics of tumour expansion more physically realistic, the model in the present paper includes the effects of mitotic inhibitors secreted from the necrotic site (as described by Freyer) in a growth retardation term of $I(n)$, assumed to be proportional to the necrotic cells density. In contrast to the model developed by Sherratt and Chaplain, the experimentally observed Gompertz growth rate is used in place of the previously employed linear representative mitosis term in the formulation of $g(c)$. Consequently, equation (1) may be modified and expressed as

$$\frac{\partial p}{\partial t} = \frac{\partial}{\partial x}\left[\frac{p}{p+q}\frac{\partial\left(p+q\right)}{\partial x}\right] + g(c)p(1-p-q-n) - \left(f(c)+I(n)\right)p \tag{5}$$

The system of equations (2)–(5) are discretized using forward differencing for time and central differencing for space. The resulting system of finite difference equations is given by

$$p_i^{j+1} = \Delta t\left[u_i^j + g(c_i^j)p_i^j\left(1-p_i^j-q_i^j-n_i^j\right) - \left(f(c_i^j)+I(n_i^j)\right)p_i^j\right] + p_i^j \tag{6}$$

$$q_i^{j+1} = \Delta t\left[v_i^j + f(c_i^j)p_i^j - h(c_i^j)q_i^j\right] + q_i^j \tag{7}$$

$$n_i^{j+1} = n_i^j + \Delta t\left(h(c_i^j)q_i^j\right) \tag{8}$$

$$c_i^j = \frac{\gamma}{\gamma+p_i^j}\left[1-\alpha\left(p_i^j+q_i^j+n_i^j\right)\right] \tag{9}$$

where

$$u_i^j = \frac{(p_{i+1}^j-p_{i-1}^j)r_i^j(r_{i+1}^j-r_{i-1}^j) + 4p_i^jr_i^j(r_{i+1}^j-2r_i^j+r_{i-1}^j) - p_i^j(r_{i+1}^j-r_{i-1}^j)^2}{4(\Delta x)^2(r_i^j)^2}$$

$$v_i^j = \frac{(q_{i+1}^j-q_{i-1}^j)r_i^j(r_{i+1}^j-r_{i-1}^j) + 4q_i^jr_i^j(r_{i+1}^j-2r_i^j+r_{i-1}^j) - q_i^j(r_{i+1}^j-r_{i-1}^j)^2}{4(\Delta x)^2(r_i^j)^2}$$

and $r_i^j = p_i^j + q_i^j$. Δt and Δx refers to the time intervals and space steps respectively in the finite difference scheme. In the above set of finite difference equations, the superscript represents the time level and the subscript represents the space position.

The experimental fit for the average cell velocity in the form of the Gamma distribution (Balazs *et al.*, 2000) led us to use a rescaled Gamma distribution term v_p, to model the random dependence of the cell proliferation rate on the cellular stress. The incorporation of the random variation in the mitosis rate due to cellular stress is according to the postulate that moderate stress promote cell division whereas low and high stress downregulate cell proliferation and promote cell death. In addition, cell velocity is assumed to correlate with the tumour expansive forces, which then contributes to the cellular stress. Hence equation (6) becomes

$$\begin{aligned} p_i^{j+1} &= \Delta t \left[u_i^j + \left(g(c_i^j) + v_p \right) p_i^j \left(1 - p_i^j - q_i^j - n_i^j \right) - \left(f(c_i^j) + I(n_i^j) \right) p_i^j \right] \\ &\quad + p_i^j \end{aligned} \tag{10}$$

The tumour is also assumed to contain several functionally-disparate clones of tumour cells, so that there exists the random collapse and regrowth of blood vessels in the tumour. In order to simulate the alternating levels of nutrients in parallel with this random variation in the tumour vascular environment, we incorporate a rescaled Normal distribution random term v_c to the quasi steady nutrient term.

Hence equation (9) becomes

$$c_i^j = v_c + \frac{\gamma}{\gamma + p_i^j} \left[1 - \alpha \left(p_i^j + q_i^j + n_i^j \right) \right] \tag{11}$$

To close the model, the following boundary and initial equations are proposed as in the model developed by Sherratt and Chaplain.

Boundary conditions at $x = 0$ and $x = 210$:

$$\frac{\partial p}{\partial x} = 0 \tag{12}$$

$$\frac{\partial q}{\partial x} = 0 \tag{13}$$

Initial conditions for $x \in [0, 210]$:

$$q(x, 0) = n(x, 0) = 0 \tag{14}$$

$$p(x, 0) = e^{-0.1x} \tag{15}$$

In the numerical solution of the finite difference equations (7), (8), (10) and (11), the parameter values as given in the model developed by Sherratt and Chaplain, are $\gamma = 10$, $c_0 = 1$ and $\alpha = 0.8$, with $f(c) = \frac{1}{2}\left[1 - \tanh(4c - 2)\right]$, $g(c) = 0.5e^{0.5c}$, $h(c) = \frac{1}{2}f(c)$ and $I(n) = \frac{1}{2}n$.

A set of random numbers for v_p from a Gamma distribution $\chi \sim Gamma(0.5, 1)$ is generated from Microsoft EXCEL 2000 before the computational process is begun. Random numbers for v_c from a Normal distribution with mean 0 and variance 0.04 are similarly obtained.

In solving the finite difference equations, Δt and Δx are set at 0.1 and 1 respectively. The code was written in Fortran and compiled and run on a Pentium 4 system. Computation was stable for the chosen set of of parameters and convergence was rapid.

3 Results and Discussion

The present model is solved for the set of parameters, functions, boundary and initial values mentioned above. Values of α values ranging from 0.05 to 0.8 were used in the simulation runs. A range of linear, quadratic and exponential functional forms for $I(n)$ were also tested. From the computational experiments, it appears that the most reasonable set of results was obtained when $I(n)$ was chosen to be a linear function, such as $I(n) = \frac{1}{2}n$. Due to space constraints, only results of the simulations for cases when $\alpha = 0.05$ and $\alpha = 0.8$ are presented and discussed here.

The results presented in Figure 2 show that the symmetry of the tumour cell distribution as observed in the model developed by Sherratt and Chaplain is broken and there is now an asymmetric spatial distribution of an advancing pulse of proliferating cells (p), with a band of quiescent cells (q) and a necrotic core (n) behind this in a radial direction at time steps $t = 0, 2, 4, ..., 14$. The predicted tumour cell distribution agrees well qualitatively with the experimental observations recorded by Dorie *et al.* (1982), which represented the internalisation of inert microspheres in multicellular spheroids.

Figure 2 demonstrates a local maximum buildup of proliferating cell density with a correspondingly lower concentration of quiescent and necrotic cell densities at the leading edge when $t = 6$. We note that as time evolves, the buildup densities of the proliferating and quiescent cells decreases whilst that of the necrotic cells increases. The space intervals between buildups of proliferating cell density is also observed to be shortened. It can be seen that with time, the outer rim of the tumour is becoming less proliferative while more and more cells undergo necrosis, resulting in a gradual deceleration of tumour growth.

Importantly, Figure 2 illustrates that the diffusion limited nutrient supply and the production of mitotic inhibitors as assumed in the model, plays a role in the observed tumour regression. Nevertheless, it is unlikely that the random pulses of high and low spatial evolution of tumour cell densities would be limited to these two factors, highlighting the importance of the random variation in the mitosis rate and nutrients level impacting its asymmetric growth.

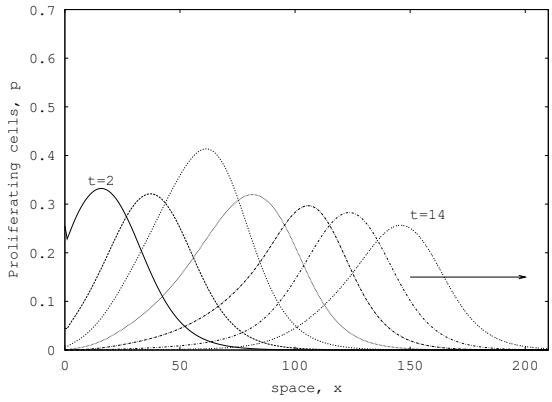

(a)

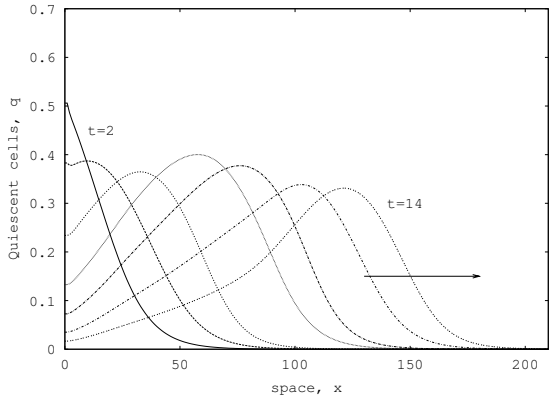

(b)

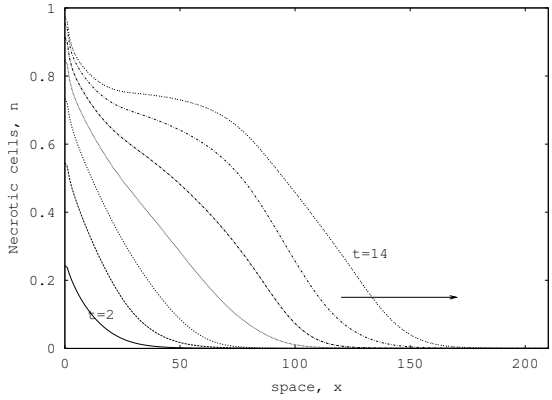

(c)

Figure 2: A numerical solution with $\alpha = 0.8$, plotted as a function of space at times $t = 0, 2, 4, ..., 14$ for (a) Proliferating cells, (b) Quiescent cells, and (c) Necrotic cells.

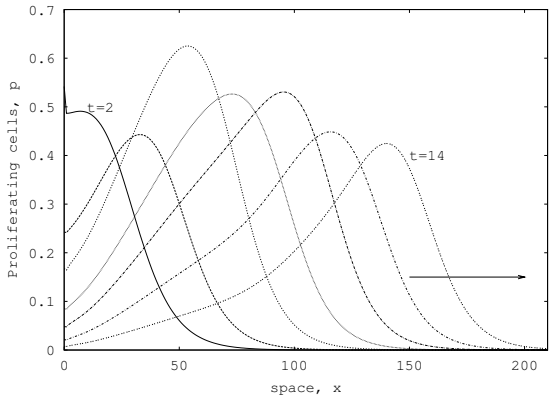

(a)

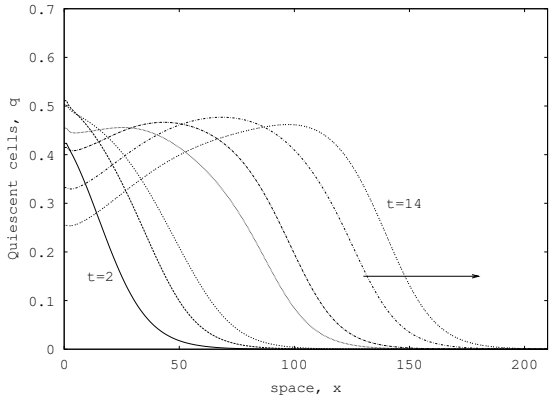

(b)

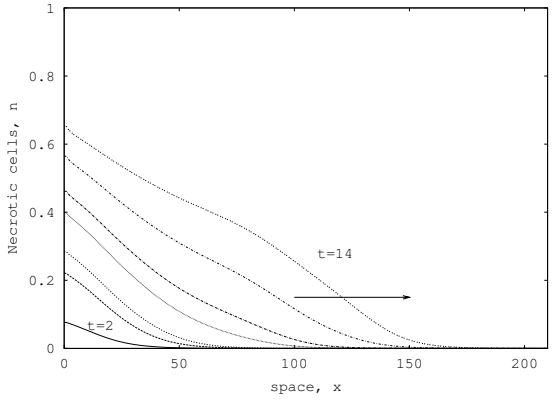

(c)

Figure 3: A numerical solution with $\alpha = 0.05$, plotted as a function of space at times $t = 0, 2, 4, ..., 14$ for (a) Proliferating cells, (b) Quiescent cells, and (c) Necrotic cells.

Figure 3 shows that as α is decreased, and hence, driven forward by the increased access of nutrient from the surrounding tissues, a larger proportion of the tumour cells proliferate, so that the layer of live tumour cells thickens and the necrotic core diminishes in size. By $t = 6$, we again see a build up of tumour cells at the leading edge, more pronounced than in Figure 3. With time, the buildup of tumour cell densities is again downregulated with no significant increase in the tumour expansion rate (This can be noticed by comparing the locations of the tumour surface).

In the current model, as can be observed from Figure 3, avascular tumour growth is shown to reach saturated growth in the absence of vascularisation. This is clearly more reasonable and realistic than the model proposed by Sherratt and Chaplain in which the simulated increased nutrient supply from the surrounding tissues is observed to be sufficient to keep all the tumour cells proliferating, with no entry into quiescence.

The tumour invasion rate is observed to be unaffected in the presence of a simulated rich supply of nutrient. Results from the present model indicate that tumour growth is influenced not only by the availability of nutrients, but also random intracellular stress effects on cell proliferation rate, v_p, as well as random variation in the nutrient level, v_c. Thus, when designing clinical intervention strategies to control tumour growth, perhaps one should consider the effects of intracellular compression on cell proliferation as these may have an impact on the overall mitotic rate.

4 Conclusion

The model presented in this paper focusses on specific aspects of tumour growth. The importance of random variation as a mechanism of asymmetric growth is obvious from these results. This in turn has made the model more realistic by considering a heterogeneous intracellular environment of the tumour. The qualitative results from the present model has provided new insights into some of the more complex physiological processes in tumour development. This model, however, may be generalised to allow for stochastic effects on the mitotic rate and nutrient level. The use of stochastic partial differential equations in such models is currently being considered by the authors. It is hoped that the results from the present model will be able to provide clinical practitioners with valuable information on the intracellular stress mechanisms and the spatio-temporal heterogeneous vascular environment that may control the development of solid tumours. These could represent future therapeutic targets to be manipulated in managing the disease.

References

1. Balazs, H., Andraz, C., Ilona, F., Tamas, M., Emilia, M. and Tamas, V.: Locomotion and proliferation of glioblastoma cells *in vitro*: statistical evaluation of videomicroscopic observations, *J. Neurosurg.*, **92**, 428–434 (2000)

2. Dorie, M. J., Kallman, R. F., Rapacchietta, D. F., Van Antwerp, D. and Huang, Y. R.: Migration and internalization of cells and polystrene microspheres in tumour cell spheroids, *Exp. Cell Res.*, **141**, 201–209 (1982)

3. Folkman, J. and Hochberg, M.: Self-Regulation of growth in three dimensions, *J. Exp. Med.*, **138**, 745–753 (1973)

4. Freyer, J. P.: Role of necrosis in regulating the growth saturation of multicellular spheroids, *Cancer Res.*, **48**, 2432–2439 (1988)

5. Helmlinger, G., Netti, P.A., Lichtenbeld, H.C., Melder, R.J. and Jain R.K.: Solid stress inhibits the growth of multicellular tumor spheroids, *Nature Biotech.*, **15**, 778-783 (1997)

6. Hystad, M. E., Rofstad, E. K.: Oxygen consumption rate and mitochondrial density in human melanoma monolayer cultures and multicellular spheroids, *Int. J. Cancer.*, **57**, 532–537 (1994)

7. Sherratt, J. A., Chaplain, M. A. J.: A new mathematical model for avascular tumour growth, *J. Math. Biol.*, **43**, 291–312 (2001)

8. Sutherland, R. M.: Cell and environment interaction in tumour microregions: The multicell spheroid model, *Science.*, **240**, 177–184 (1988)

9. Ward, J. P., King, J. R.: Mathematical modelling of avascular tumour growth, *IMA J. Math. Appl. Med. Biol.*, **14**, 39-70 (1997)

10. Ward, J. P., King, J. R.: Mathematical modelling of avascular tumour growth, *IMA J. Math. Appl. Med. Biol.*, **16**, 171–211 (1999)